

Structure Optimization of Ultra-Light Power Generation System

Pingping Wen ^{1,2}, Zhibao Yuan ¹, Haiping Xu ¹ and Zengquan Yuan ^{1,*}

¹ Institute of Electrical Engineering, Chinese Academy of Sciences, Beijing 100190, China; wenpingping@mail.iee.ac.cn (P.W.)

² University of Chinese Academy of Sciences, Beijing 100049, China

* Correspondence: zengquanyuan@mail.iee.ac.cn

Abstract: A wide-speed, ultra-light power generation system is a critical power generation unit structure, often because of its high efficiency and power density. Lightness and reliability are two key design indicators within the system, albeit they could lead to contradictory problems, particularly in systems containing prime movers, batteries, generators, rectifiers, and inverters. Ultra-light generator sets are facing more severe problems and contradictions in designing in terms of matching, coordinating, and stabilizing the components in the systems. This paper describes the system design of a low-cost and high-reliability microgenerator set: a gasoline engine, three-phase permanent magnet synchronous generator, rectifier, and inverter. Moreover, the matching relationship between the four parts and the design effect of each part of the power generation system was analyzed, simulated, and tested to verify the effectiveness and feasibility of the so-designed system.

Keywords: ultra-light power generation; miniature gasoline engine; generator winding design; rectifier; series power generation topology

1. Introduction

Ultra-light power generation equipment (ultra-light power plant) has high requirements in power density, continuous operation, and transient stability of the entire machine. There is also a direct conflict between the design of high power density and substantial stability control in the creation of power units. Considering that the ultra-light power station needs to meet the power density requirements when designing the power unit (engine-generator), the rated speed of the power unit is higher, and the speed regulation range is more extensive, which increases the difficulty of the power and speed control of the power unit and the control of the whole machine condition, especially for the load mutation condition. Therefore, a feedforward control strategy for the power unit of ultra-light power generation equipment is proposed to improve the load-switching response. The power unit control strategy experiment of ultra-light power generation equipment was conducted to verify the effectiveness and efficiency of the proposed control strategy [1–8].

A permanent magnet synchronous generator (PMSG) has many advantages, such as high efficiency, high power density, flexible topology, no brush mechanism, etc. Therefore, it is increasingly widely used on many occasions, such as in wind turbines [9–13], gas turbine generators [14], aerospace main generators [15], vehicle generators or starting/generating units [16–18], and flywheel energy storage system electric/generating units [19], and covers a wide range of power from megawatts to watts. The engine and the generator coaxially connect the power unit, so the control of the power unit is mainly reflected in the management of the engine:

The topological division and selection basis of ultra-light power generation equipment in multi-machine and single-machine systems are analyzed.

The physical and mathematical models of the engine are discussed and the relationship of external characteristics is interpreted.



Citation: Wen, P.; Yuan, Z.; Xu, H.; Yuan, Z. Structure Optimization of Ultra-Light Power Generation System. *Energies* **2024**, *17*, 976. <https://doi.org/10.3390/en17050976>

Academic Editors: Omar Ali Beg, Shan Zuo and Zongjie Wang

Received: 18 September 2023

Revised: 25 November 2023

Accepted: 10 December 2023

Published: 20 February 2024



Copyright: © 2024 by the authors. Licensee MDPI, Basel, Switzerland. This article is an open access article distributed under the terms and conditions of the Creative Commons Attribution (CC BY) license (<https://creativecommons.org/licenses/by/4.0/>).

According to the load-switching response speed requirements, the load current is introduced into the control loop as the feedforward quantity. The power chain's peak speed limit is considered to prevent the car from stalling and ensure the unit runs for a long time.

The theoretical model was verified through the power unit test experiment to obtain the measured external characteristic curve of the engine.

The permanent magnet synchronous generator itself outputs alternating current. The output frequency of the generator is stable only when the prime mover speed is constant, but the output voltage still varies with the load. To reduce the voltage adjustment rate when designing the generator, it is often necessary to significantly increase the permanent magnet load to reduce the number of turns and impedance of the winding. Therefore, the magnetic load and the electrical load may be uneven, which has a negative impact on the power density and cost of the generator. Moreover, the prime mover often has variable speed operation, and even if the speed range is extensive (for example, the speed of the vehicle generator can change by more than ten times [20]), the output frequency and voltage of the generator are unstable. Therefore, permanent magnet synchronous generators usually require AC–AC or AC–DC–AC power electronic devices to achieve AC voltage regulation and constant frequency and can also reach AC grid connection. In the actual system, an AC–DC–AC structure is the most common. Of course, permanent magnet synchronous generators can also provide DC power through AC–DC devices (such as automotive generators). If necessary, DC–DC devices can achieve high-quality DC voltage regulation.

Therefore, most practical applications of permanent magnet synchronous generators require a set of power electronic devices to achieve rectification and voltage regulation (that is, to provide a stable DC power supply), thus forming a basic generator system. Common types of rectifiers and DC voltage regulation include thyristor-controlled rectifiers, diode-uncontrolled rectifiers + DC–DC conversion, and PWM rectifiers [21]. If an AC power supply or AC grid connection is required, the inverter can be connected after the DC link. Of course, the inverter can stabilize the AC side voltage, so the requirements for front-end DC voltage regulation are relatively low.

For the primary permanent magnet synchronous generator system with variable speed and variable load, the voltage regulation control includes two categories: the generator's output voltage is not stable, but the DC voltage is challenging, called single-port voltage regulation. The output end of the generator is regulated, and the DC end is controlled, called dual-port voltage regulation. This paper will analyze and design the structure and topology of these two kinds of systems.

In this paper, the topology scheme of the whole system and the scheme of multi-machine expansion are carefully described, along with the model of the engine and comparisons of different converter schemes. The generator, rectifier, and the double buck inverter are presented as both a model and in-depth analysis. The results of the simulation and experiment prove that the so-modeled system exhibits high efficiency, reliability, and is low cost. Engine and generator coaxial connection structure diagram, physical diagram of the generator rotor, permanent magnet synchronous motor load density cloud and load magnetic field line distribution simulation, actual drawing of the whole power generation system platform, engine external characteristic test platform are shown in Appendix A.

2. System Topology and Structure Design

Similar to traditional power stations, the whole system of ultra-light power stations is mainly composed of two parts: a power unit and a converter unit. However, for long-term stability, it does not include an energy storage unit. Among these, the power unit comprises the engine and the generator, two parts of a mechanical coaxial connection, and the engine is the prime mover through the coaxial drive generator's automatic movement. The generator is responsible for converting the exceptional power into electrical energy. The converter unit has different converter forms according to additional output electrical energy requirements, responsible for various forms of electrical energy conversion. Depending on the power level and demand occasions, the engine can choose a Stirling machine, gas turbine, diesel

engine, gasoline engine, etc. At the same time, the generator can be considered a permanent magnet motor, electric excitation generator, or hybrid excitation generator [4,5]. Common power station system structure as shown in Figure 1.

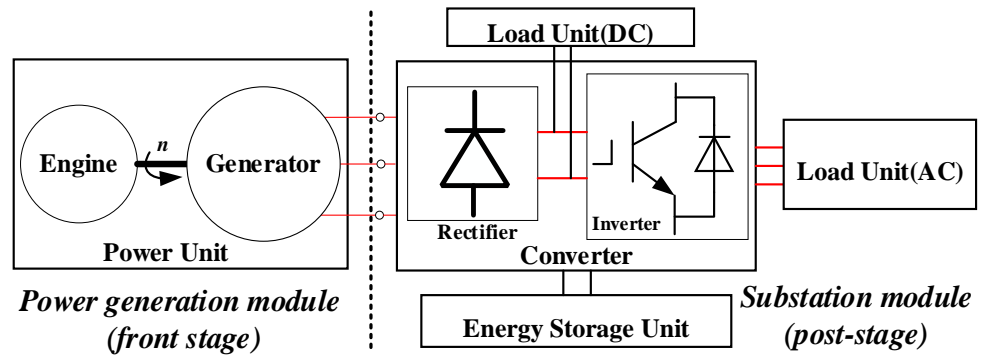


Figure 1. Configuration of power station common system.

When considering the topology design of the power station, based on the possibility of port expansion, it can be divided into the standard DC bus topology scheme, as shown in Figure 2a, and the classic AC bus topology scheme, as shown in Figure 2b. In the DC bus scheme, each power unit selects the output DC for multi-machine parallel, then converts the external power frequency power output. In contrast, in the standard AC bus scheme, each power unit independently performs the rectification and inverter process, and then selects the power frequency output end to directly parallel the power supply to the load.

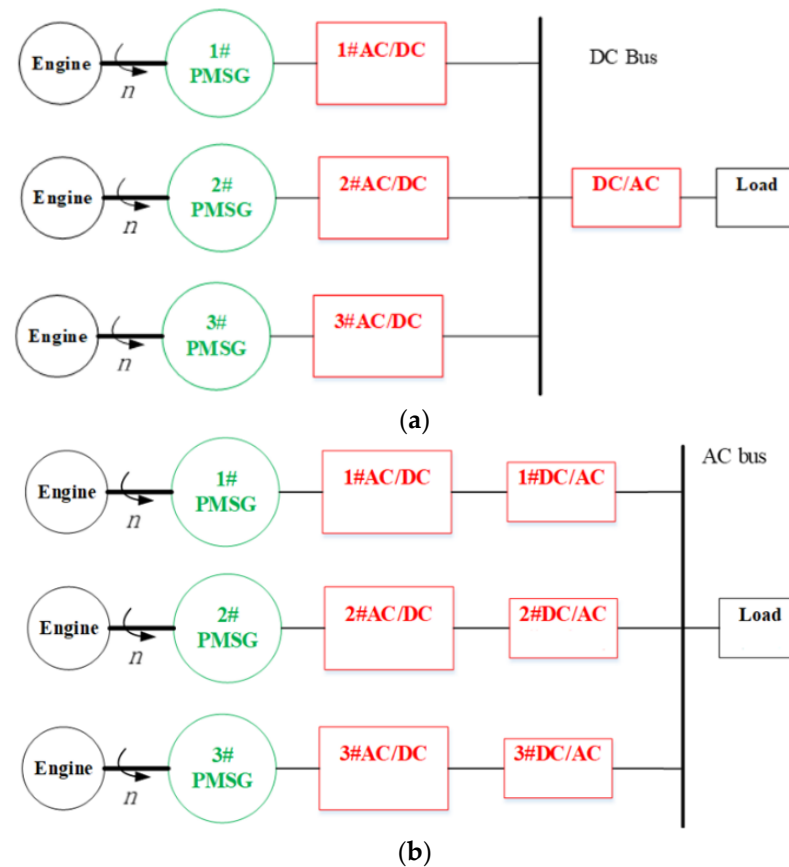


Figure 2. Multimachine extension topology of power plant system. (a) DC bus topology scheme; (b) AC bus topology scheme.

The two parallel expansion schemes have advantages and disadvantages. Considering the stability problems caused by the increased coupling between the whole machine driven by the inverter in the DC bus scheme as a common inverter unit, the AC bus parallel scheme can consider the parallel connection without interconnection based on independently completing the inverter output, increasing the expansion and stability of the system while reducing the coupling degree between the whole machine.

When the AC bus scheme is adopted, the power unit control of each subunit is relatively independent and flexible. Considering a single power station, a series non-energy storage unit system structure is directly composed of a miniature gasoline engine, a multi-winding permanent magnet synchronous generator, a three-phase rectifier, and a single-phase inverter in a chain structure, as shown in Figure 3 below.

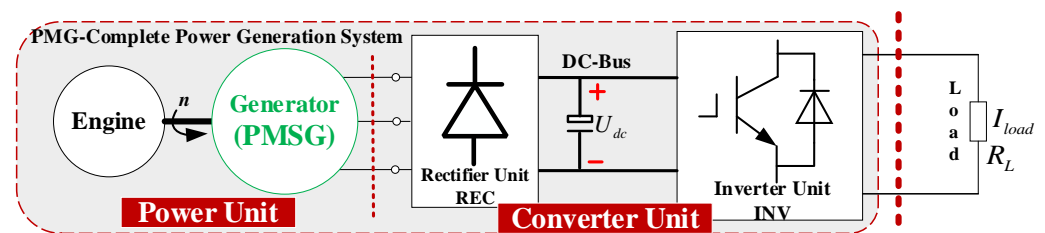


Figure 3. Plant system structure diagram of cascade type non-energy storage unit.

3. Model Analysis and Improvement Design of Selected Engine

3.1. Engine Modeling Analysis

The main requirement for a light mobile power system is to provide as much mechanical power as possible in the smallest possible size and weight. It should also have high fuel economy and oil efficiency, as well as increased operational reliability. According to the small capacity power characteristics of the light mobile power system, the engine options to be considered are (1) micro gas turbine, (2) micro diesel engine, (3) small gasoline engine, and three other engine options.

The light mobile power generation mainly uses a gasoline engine with higher speed and lifting power, and relatively good torque adaptability, lighter mass, smaller size, low vibration, and noise. Therefore, it is more suitable for the prime mover solution of an ultra-light mobile power generation system.

The energy conversion and power generation involved in a gasoline engine's operation are complex, non-electrical processes. The process includes air intake, fuel injection, ignition, combustion, and exhaust. At the same time, this kind of engine often faces special transient conditions when working, such as starting and stopping, sudden loading and unloading. When the temporary load changes, the internal thermal stability state of the engine will change due to the thermal inertia lag of the relevant stroke-executing components. For example, the formation of a mixed gas in the engine cylinder will also be affected by the inertia of the liquid fuel, which is more significant than the air, resulting in the engine becoming thinner in the mixture during sudden load reduction, and the acceleration response becomes worse, resulting in a shutdown. When it works under unstable conditions, it is difficult to establish an accurate mathematical model that can be used for real-time control.

When the load torque of the engine (the electromagnetic torque of the generator is the load torque of the engine) is constant without other factors, it can be regarded as working under stable conditions, which can be expressed under the given load torque:

$$T_{Eng} - T_e = J \frac{d\omega_{Eng}}{dt} \quad (1)$$

where ω_{Eng} is the engine angular velocity (rad/s); J is the moment of inertia of the engine output shaft; T_{Eng} is the engine output dynamic torque; T_e is the load torque. If the load is unchanged and only the input (carburetor opening θ) changes, then the following formula applies:

$$\begin{cases} T_{\alpha}^* \frac{d\varphi}{dt} + S_{\delta} = \kappa_{\theta} \cdot \theta \\ \varphi = \kappa_{\eta} \cdot (1 - e^{-\frac{S_{\delta}}{T_{\alpha}^*}}) \\ S_{\delta} = \frac{\omega}{T_{REng}} \cdot (\frac{\partial T_e}{\partial \omega} - \frac{\partial T_{Eng}}{\partial \omega}) \end{cases} \quad (2)$$

where T_{α}^* is the response time constant of the engine (that is, the time required for the engine to start to the rated working condition when the carburetor opening is at a particular fixed power/torque value under no-load conditions).

According to Formulas (1) and (2), when the load is unchanged, the speed and carburetor opening are first-order relations, and the transfer function can be obtained:

$$G^*(s) = \frac{\varphi(s)}{\theta(s)} = \frac{\kappa_{\theta}}{T_{\alpha}^*s + S_{\delta}} \quad (3)$$

When considering the power model with pure hysteresis, we can obtain:

$$G(s) = \frac{\kappa_1}{T_{\alpha}s + 1} \cdot e^{-\tau s} \quad (4)$$

Only the load torque is considered if the engine carburetor opening is unchanged. This is because the relationship between the generator’s electromagnetic torque change and the engine speed change is not part of the engine speed feedback loop. Thus, at this time, the dynamic characteristic transfer function between the load torque (here, it is also the electromagnetic torque of the generator) and the engine speed is:

$$G_{LT}(s) = \frac{\kappa_2}{T_{\beta}s + 1} \quad (5)$$

When the engine is working under unstable conditions, such as sudden load changes, it is difficult to establish an accurate mathematical model, and a relatively accurate mathematical model can be obtained by combining experimentation and transient theoretical analysis. External torque characteristics of engine and generator as shown in Figure 4 below.

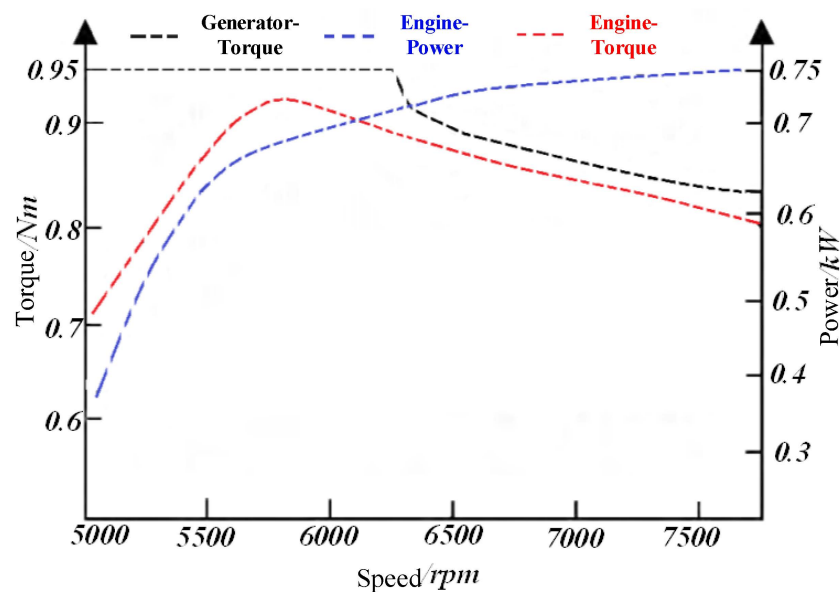


Figure 4. External torque characteristics of engine and generator.

3.2. External Engine Characteristics and Analysis

The comparison diagram of the torque external characteristic curves of the engine and generator mentioned above is qualitatively obtained based on the design. The torque characteristics and power characteristics of the engine are coupled with each other and exhibit complex nonlinear characteristics. Further, by measuring the torque–tach–power characteristic data of the micro-engine through the eddy current power measuring platform, the engine’s mathematical model can be optimized, which provides a basis for analyzing the speed instability condition of the power unit and designing the speed stability control strategy. Fitting results of three-dimensional curve among engine throttle opening, speed, and torque as shown in Figures 5 and 6 below.

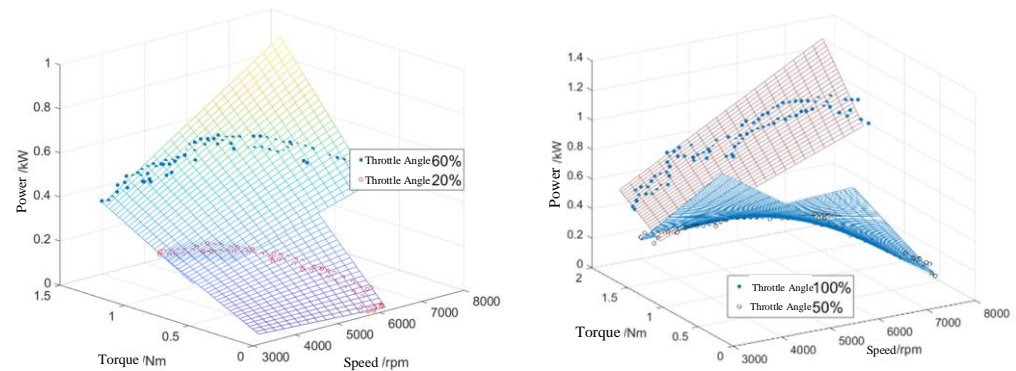


Figure 5. Fitting results of three-dimensional curve among engine throttle opening, speed, and torque.

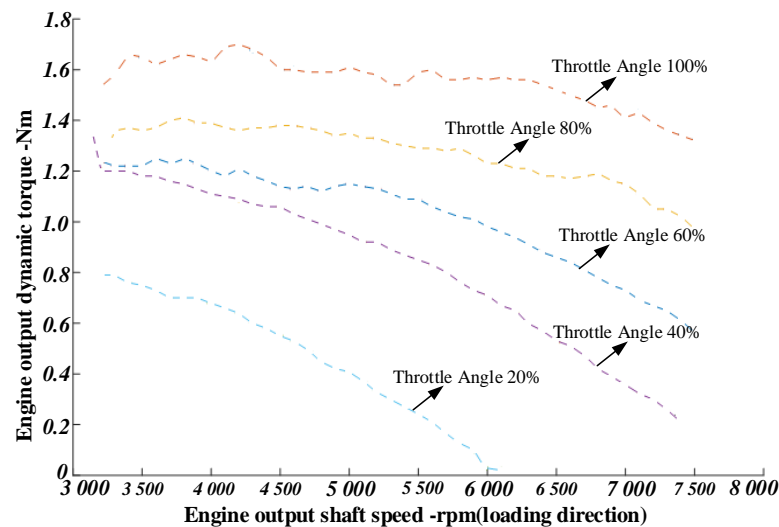


Figure 6. Speed–torque relationship curve.

3.3. Modification of Engine Stall Restrictions

The speed limit stability control is mainly aimed at preventing excessive speed (more than 10,000 rpm) caused by sudden load reduction when the load changes. Due to the strong integration of the engine and generator, the output voltage of the generator under the speed limit becomes too high, which can lead to breakdowns in the after-stage converter unit. Therefore, it is necessary to impose a speed limit, which is implemented by the ignition unit of the engine. The engine TCI ignition scheme design is shown in Figure 7 below. Because there is no energy storage unit in the ultra-light power station, choosing the high-voltage lighter package scheme is impossible. Instead, select a hand-pulled generator to start the ignition, and the generator design table is equipped with a permanent magnet for ignition and an accompanying ignition winding.

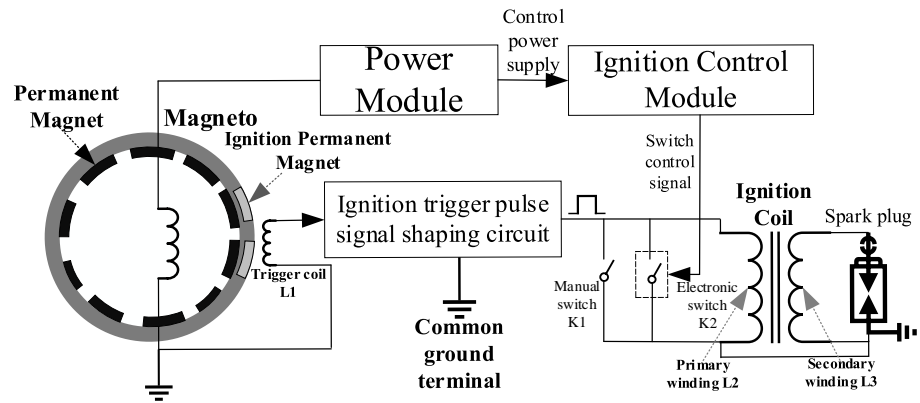


Figure 7. Schematic diagram of engine TCI ignition scheme.

The response of the power unit output shaft speed for the engine ignition speed limit and throttle adjustment is shown in Figure 8 below. The trigger point of speed can be adjusted by adjusting the ignition angle and winding state.

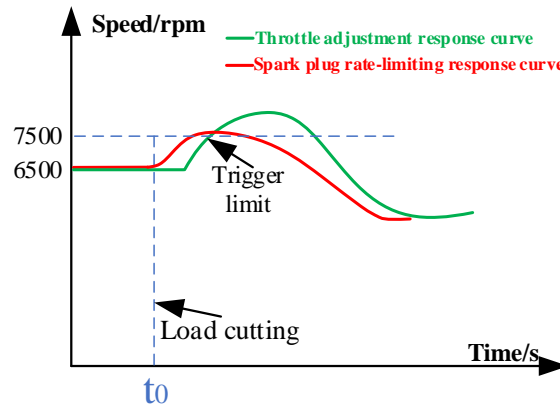


Figure 8. Schematic diagram of engine ignition speed limiting principle.

In summary, the timing sequence of the load switching response speed regulation strategy of the power unit, considering the speed feedback PID closed-loop control of the output shaft of the power unit, the load current feedforward control, and the ignition speed limiting control, is shown in Figure 9. Among them, the ignition flameout speed-limit trigger point is 8000 rpm, and the feedforward trigger current limit value of the load current is 0.3 A (15% load current increment).

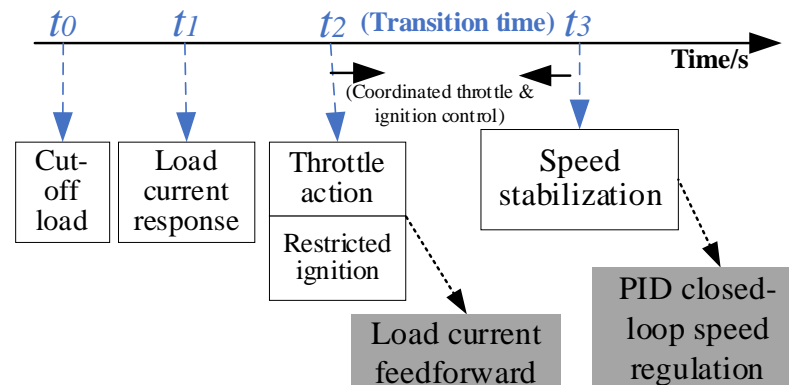


Figure 9. Power unit integrated control time sequence.

4. Topology Scheme and Model Analysis of Generator Side Voltage Regulation

4.1. Motor Types and Modeling Analysis

Many types of motors can be used as generators in DC energy systems. For example, synchronous motors include electrically excited synchronous machines (EESM), permanent magnetic synchronous motors [12], hybrid excited synchronous machines (HESM) [1–4], induction machines (Induction Machine, IM), switched reluctance motors (Switched Reluctance Machine, SRM), etc. Many scholars have studied the system performance (stability and dynamics) and control methods of induction generators (IG) used in wind power generation, automotive power generation, aircraft power generation systems, and other applications. Its beneficial characteristics include low cost, high reliability, and robustness.

In recent years, the use of permanent magnets has become very attractive due to the improvement of their performance and the reduction in their cost. On the other hand, with the progress of power electronics technology, sensor technology, control technology, large-scale integrated circuits, and other related technologies, the performance of permanent magnet motors has been dramatically improved. Permanent magnet synchronous motor (PMSM) and permanent magnet synchronous generator (PMSG) with its high power density, efficiency, and reliability, PMSG is an excellent model for various industrial applications. Therefore, permanent magnet motors, together with full-power converters, are becoming more and more attractive and are increasingly being applied. The advantages of permanent magnet synchronous generators compared with electrically excited synchronous generators and doubly fed induction generators can be summarized as follows: ① higher efficiency, ② no additional excitation power supply, ③ improved thermal characteristics, ④ higher reliability, ⑤ lighter weight, higher power density. However, a permanent magnet synchronous generator has a constant magnetic excitation flux linkage. Because of the danger of demagnetizing permanent magnets, achieving the weak magnetic regulation required by a high-speed working area is not easy in a permanent magnet synchronous motor.

The generator studied in this paper is a surface-mounted six-phase PMSG. Because of the multi-winding structure and the three-phase primary winding as its central part, the six-phase motor can be simplified into a three-phase motor for modeling analysis and discussion. The structure diagram of the five-pole six-phase PMSG is shown in the figure below, and the phase windings are evenly distributed by 60° on the stator circumference. Take the phase around the axis as the origin, and the space angle of any position on the inner circle of the stator in the counterclockwise direction is θ . As shown in Figure 10, the generator has different specific forms of winding and its simplification into three-phase winding. As shown in Figure 11, the generator has three sets of specific forms corresponding to different functions: (1) the primary winding for AC power output; (2) ignition winding for engine ignition; (3) auxiliary winding for direct current and other purposes.

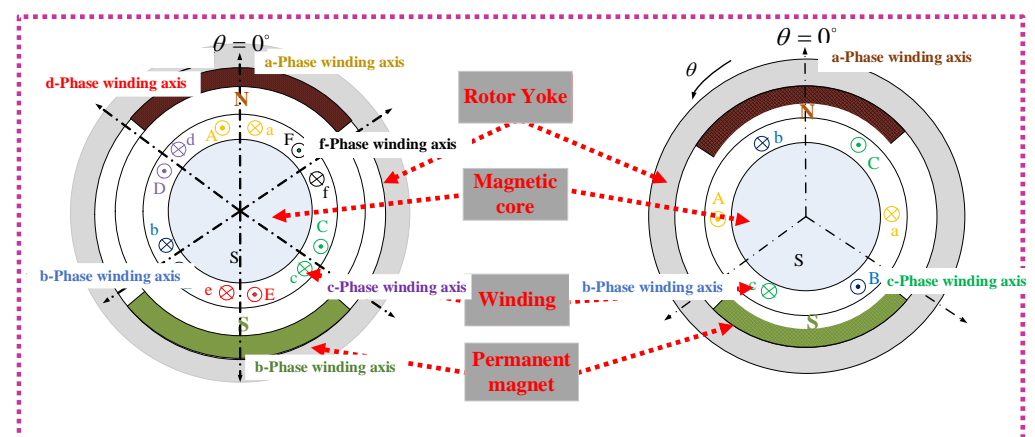


Figure 10. Six-pole-multi-winding PMSG.

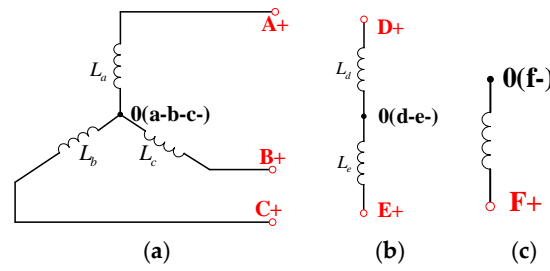


Figure 11. Multi-winding distribution of permanent magnet synchronous motor. (a) Three-phase main winding; (b) ignition winding; (c) auxiliary winding.

For the simplification of the physical model, the following assumptions are made:

- (1) The influence of other harmonic components is ignored in the stator winding and permanent magnet flux linkage of the motor.
- (2) The magnetic circuit of the motor is linear, without considering the influence of core saturation, hysteresis, and eddy current effects.
- (3) Regardless of the influence of the stator surface teeth and slots, there is no damping winding on the rotor.

In summary, the generator voltage equation can be analyzed:

$$\begin{cases} V_d = -(R_s i_d + L_d \frac{di_d}{dt}) + \omega_e L_q i_q \\ V_q = -(R_s i_q + L_q \frac{di_q}{dt}) - \omega_e L_d i_d + \omega_e \psi_{mf} \end{cases} \quad (6)$$

where a and b are stator d axis and q axis voltages, respectively; c and d are stator d axis and q axis currents, respectively; e is the stator resistance of PMSG; f is the excitation flux produced by the rotor permanent magnet in the armature winding; g and h are the inductance of stator d axis and q axis, respectively; i is the electrical angle of the rotor; j in the d - q axis coordinate system, the motor back electromotive force is represented as k and m. Equivalent diagram for a three-phase PMSG vector is as shown in Figure 12. And the Designing parameters of PMSG in the model experimental test is as shown in Table 1.

Electromagnetic torque equation:

$$T_e = \frac{3}{2} p [\psi_{mf} + (L_q - L_d) i_d i_q] \quad (7)$$

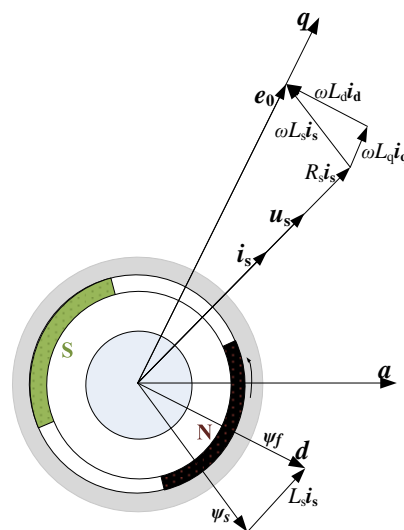


Figure 12. Equivalent diagram for a three-phase PMSG vector.

Table 1. Designing parameters of PMSG in the model experimental test.

Parameters	Value	Parameters	Value
Stator equivalent inductance L_d /(mH)	7.79	Number of poles	5.0
Stator equivalent resistance/(Ω)	5.84	Rotor equivalent resistance/(Ω)	3.89
Rated speed/(rpm)	7000	Rated torque/(N·m)	0.5
Rotor equivalent inductance L_d /(mH)	7.79	Mutual inductance/mH	0.39
Permanent magnet flux linkage ψ_f /(Wb)	0.59	Moment of inertia/(kg·m ²)	0.008

4.2. Motor Output Rectifier Scheme Selection

Power electronics technology plays an essential role in integrating renewable energy systems and the design of generator systems. The AC power generated by the permanent magnet synchronous generator is converted into direct current by an AC/DC converter. AC/DC converters, also known as rectifiers, come in some significant types, such as diode rectifiers, thyristor rectifiers, and PWM rectifiers. Due to the unpredictability of the speed of the prime mover, the generators used in the studied DC electric energy system generally work under variable speeds. Different AC/DC converter topologies have different effects on motor selection, system control, and performance [14]. Several mainstream rectification topologies are shown as in Figure 13. Comparison of topological characteristics of power converter is as shown in Table 2.

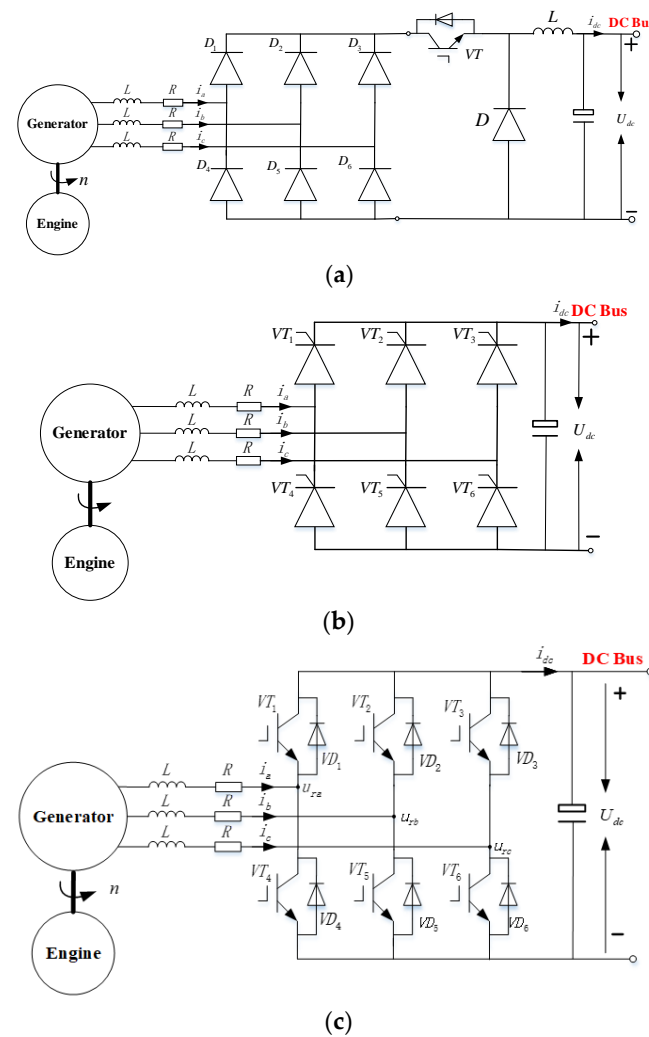


Figure 13. Several mainstream rectification topologies. (a) Diode–Buck rectifier program; (b) Thyristor rectifier program (SCR); (c) PWM rectifier program.

Table 2. Comparison of topological characteristics of power converter.

Converter Topology	Main Characteristics
Diode + Buck converter	<ol style="list-style-type: none"> 1. Low price (diode); 2. High quality DC bus; 3. The voltage level is determined by CEMF.
Thyristor rectifier	<ol style="list-style-type: none"> 1. Low price, wide use; 2. Large fluctuation of DC bus (low quality); 3. The voltage level is determined by CEMF.
PWM rectifier	<ol style="list-style-type: none"> 1. The voltage level is determined by the DC bus voltage; 2. Simple structure.

The diode rectifier belongs to the early rectification scheme. The output voltage is not adjustable, and a regulator has manual voltage regulation, poor dynamic response, significant losses, and other shortcomings; even with the addition of a buck circuit, there is still the problem of a small voltage regulation range. Thyristor rectifiers can overcome the shortcomings of diode rectifiers with the advantages of a large capacity and a wide power range. While the switching rectifier can reasonably achieve the rectification effect, the cost is very high. Therefore, due to the high-reliability requirements of the occasion and low-cost control, the final choice is the thyristor rectifier.

4.3. Topology Design and Parameter Design of AC Output Inverter

The inverse converter is regarded as an important element in electro-electronic technology. It is widely used in modern intelligent power networks and energy source power generation systems, where the “transmission bridge inverter” is located in the upper and lower bridge arms with high-frequency switching tubes. It is necessary to add a dead zone time between the opening and closing signals of the upper and lower bridge arms. The bridge inverter continues to conduct on the body diode of the opening and closing tube, and the reverse recovery time is long, which will create large opening and closing losses. The increase in the switching frequency and efficiency of the inverter system is limited.

The double Buck inverter is a toppling structure studied and widely used in recent years. Its basic circuit unit is the Buck circuit, where the switching tube and the diode tube are connected in series to form the current bridge arm. The problem that does not exist in the high-frequency switching tube is more reliable than that of the transmission bridge inverter. In addition, the double Buck inverter uses the Buck circuit diode instead of the body diode of the switch tube as the output continuous current, which reduces the output inductive current commutation time and reduces the reverse recovery losses. This can help improve the system’s switching frequency and efficiency.

A dual Buck inverter consists of two sets of identically symmetrical Buck circuits, as shown in Figure 14 and the equivalent model of dual Buck inverter is shown as in Figure 15. u_d is the input power supply, u_C is the filter capacitor voltage, i_{L1} and i_{L2} are the currents of the filter inductor L1 and L2, i_o is the load current, and C_o , L1, and L2 constitute the low-pass filter. Because of the existence of power devices, the inverter is essentially a nonlinear system. Assuming that the input voltage is constant, the power tube is an ideal device, and the switching frequency is much higher than the output fundamental frequency of the inverter and the resonant frequency of the LC filter, the approximate model of the inverter can be simplified as shown in Figure 16. Physical diagram of the main circuit and controller of the inverter is shown as in Figure 17.

u_d is a voltage pulse sequence with amplitude $\pm u_d$, $L = L1 = L2$. Taking inductance current i_L and capacitance voltage u_C as state variables, the equation for the small signal state of dual Buck inverters is:

$$\begin{pmatrix} \dot{i}_L \\ \dot{u}_C \end{pmatrix} = \begin{pmatrix} \frac{1}{L}u_d - \frac{1}{L}u_C \\ \frac{1}{C}i_L - \frac{1}{RC}u_C \end{pmatrix} \quad (8)$$

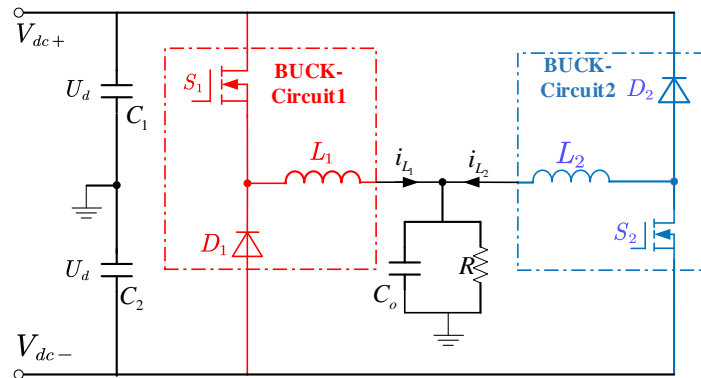


Figure 14. Main circuit of dual Buck inverter.

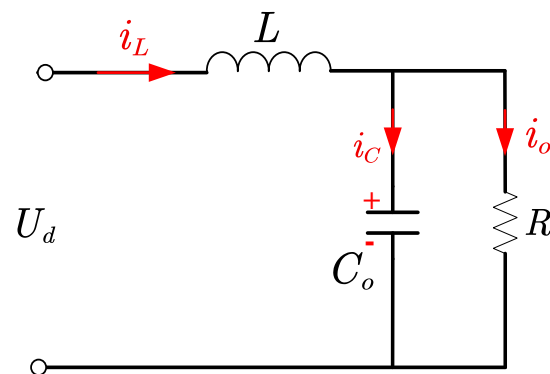


Figure 15. Equivalent model of dual Buck inverter.

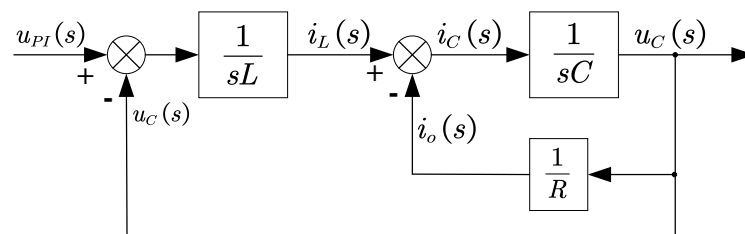


Figure 16. Block diagram of the main circuit system.

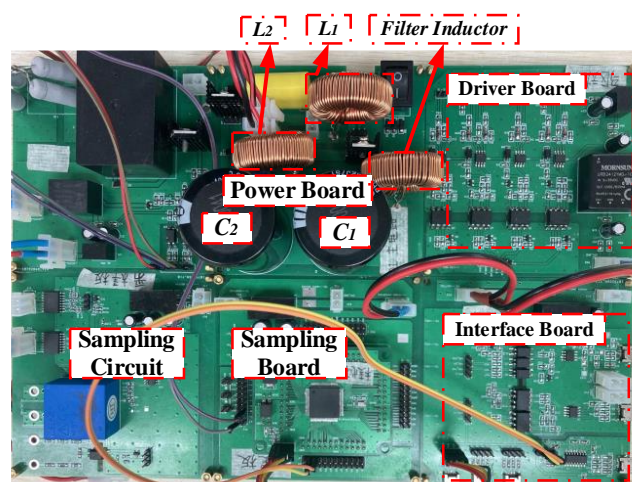


Figure 17. Physical diagram of the main circuit and controller of the inverter.

Write the inverter’s small signal equation as a standard mode (distinguish state quantity and control quantity):

$$\begin{bmatrix} \frac{d\hat{i}_L(t)}{dt} \\ \frac{d\hat{u}_C(t)}{dt} \end{bmatrix} = \begin{pmatrix} 0 & -\frac{1}{L} \\ \frac{1}{C} & -\frac{1}{RC} \end{pmatrix} \begin{pmatrix} \hat{i}_L(t) \\ \hat{u}_C(t) \end{pmatrix} + \begin{pmatrix} \frac{1}{L} \\ 0 \end{pmatrix} \hat{u}_d(t) \tag{9}$$

According to the small signal equation of state, the transfer function between inductance current and control quantity (PWM) is obtained (small signal premise):

If the filter capacitor equivalent series resistance r is considered, the open-loop transfer function of the main power loop can be written as:

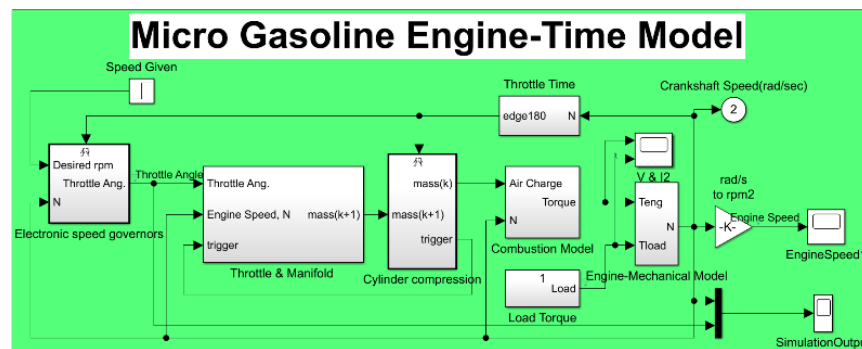
$$G_{vd}(s) = U_d \frac{1 + \frac{s}{\omega_{esr}}}{1 + \frac{s}{\omega_o Q} + \left(\frac{s}{\omega_o}\right)^2} = U_d \frac{1 + Cr_{esr} \cdot s}{1 + \frac{L}{R} \cdot s + LC \cdot s^2} \tag{10}$$

Buck circuit small signal transfer function:

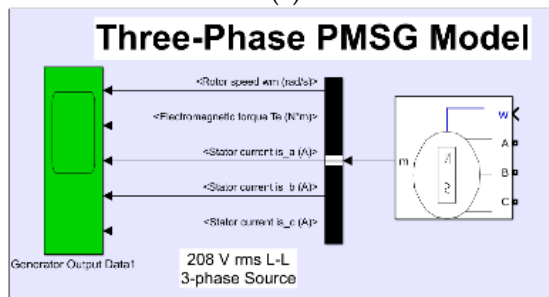
$$G(s) = \frac{u_{fbk}(s)}{u_{Ctrl}(s)} = G_{vd}(s) \cdot G_{pwm_gen}(s) \cdot G_{fc} = \frac{u_C(s)}{u_{d_pwm}(s)} \cdot \frac{u_{d_pwm}(s)}{u_{Ctrl}(s)} \cdot \frac{u_{fbk}(s)}{u_C(s)} \tag{11}$$

5. Simulation and Machine Experimental Result

Simulation is conducted for small gasoline engines, three-phase thyristor bridge rectifier circuits, and single-phase inverters to model and analyze the system. The effectiveness and stability of the designed system can be determined by observing the engine’s change process. System program simulation structure is shown as in Figure 18.



(a)



(b)

Figure 18. Cont.

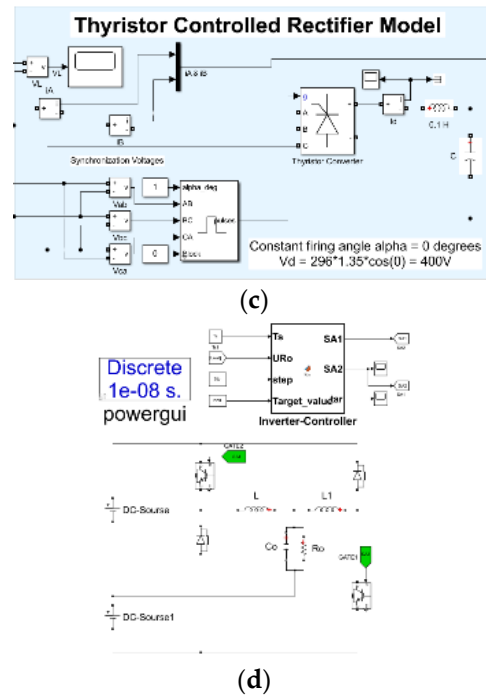


Figure 18. System program simulation structure. (a) Engine module; (b) generator module; (c) rectifier module; (d) inverter module.

The prime mover of the ultra-light power generation system, using a series engine and a coaxial link generator without energy storage, is a miniature gasoline engine with high speed and small inertia. The speed response curve of its closed-loop and open-loop control is shown below. The experimental results show that the engine, with high speed and low inertia, cannot recover the required speed without closed-loop control, and the speed is 30% lower (at 100% load), which means that sufficient generating speed cannot be guaranteed. Therefore, closed-loop control must be adopted. Open-loop and closed-loop engine speed response is shown as in Figure 19.

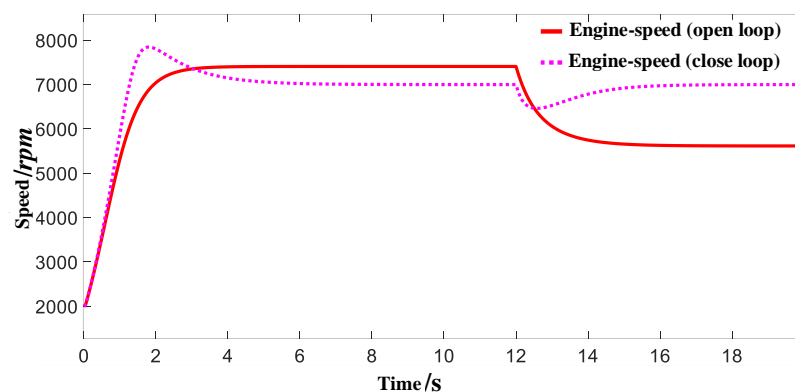


Figure 19. Open-loop and closed-loop engine speed response.

The output voltage simulation and actual experimental results of the three-phase main winding of the generator are shown as follows. According to the results of simulation and platform experiments, the generator winding scheme designed in this paper can guarantee the power output with a good sinusoidal degree (less than 5% THD) and the maximum efficiency output (94% efficiency) over a wide speed range. Since the rated speed of the generator designed in this paper is twice that of the same kind of motor, it can also effectively improve the power density of the generator and the whole system, with an average increase of 45%. Light load generator phase voltage waveform is shown as in Figure 20.

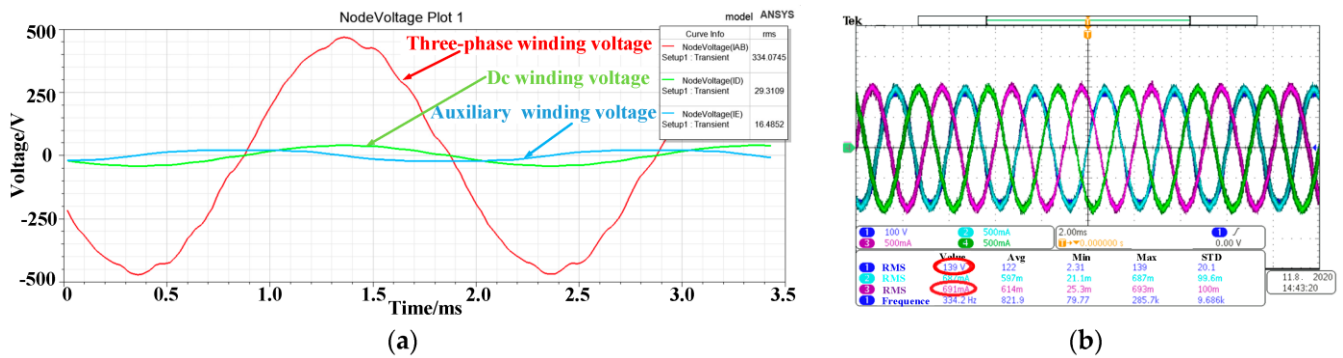


Figure 20. Light load generator phase voltage waveform. (a) Three-phase/DC/auxiliary winding voltage (simulation); (b) three-phase winding voltage (Real).

6. Conclusions

This paper first points out several key steps in ultralight generator system design: prime mover selection and working principle analysis, generator modeling and winding design analysis, rectifier components, and topology selection and analysis. According to the two important design requirements of an ultra-light power generation system for high power density and high stability, the need for high power density makes the rated speed of the generator higher than the ordinary generator speed, and the need for high stability makes the devices used in the rectifier circuit need to be more resistant to high voltages. Finally, a small gasoline engine is determined as the prime mover of the power generation system, a multi-winding six-phase permanent magnet synchronous motor is used as the generator part of the generator system, and a three-phase thyristor bridge circuit is used as the rectifier part of the power generation system. Finally, the simulation design of the micro-power generation system is carried out to verify the effectiveness, low cost, and high reliability of the designed scheme.

Author Contributions: Conceptualization, P.W.; methodology, P.W.; software, P.W.; validation, Z.Y. (Zhibao Yuan) and H.X.; formal analysis, P.W.; investigation, P.W.; resources, P.W.; data curation, P.W.; writing—original draft preparation, P.W.; writing—review and editing, P.W.; visualization, Z.Y. (Zhibao Yuan); supervision, Z.Y. (Zengquan Yuan); project administration, Z.Y. (Zengquan Yuan); funding acquisition, Z.Y. (Zengquan Yuan). All authors have read and agreed to the published version of the manuscript.

Funding: This work was supported by Research Fund of Institute of Electrical Engineering, Chinese Academy of Sciences (E21Z350101).

Data Availability Statement: Data is contained within the article.

Conflicts of Interest: The authors declare no conflict of interest.

Appendix A

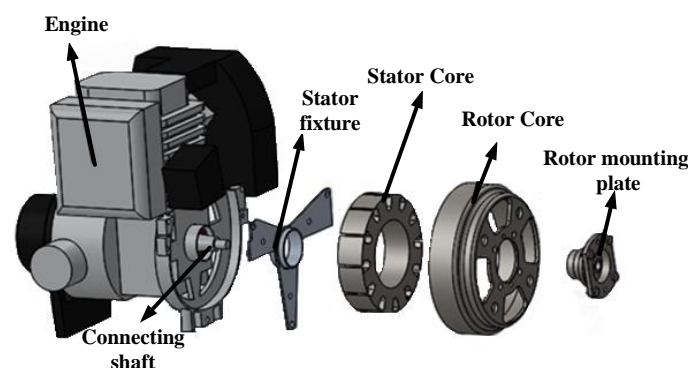


Figure A1. Engine and generator coaxial connection structure diagram.



Figure A2. Physical diagram of the generator rotor (left) and structural design diagram of the stator (middle) and physical diagram (right).

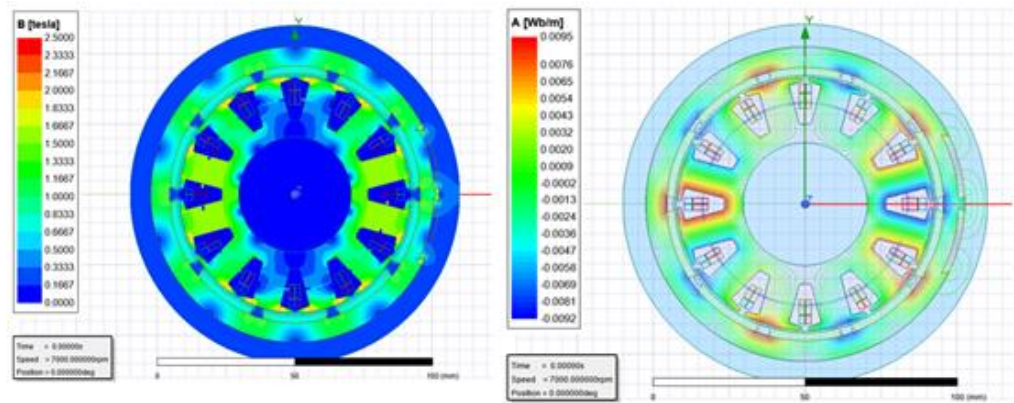


Figure A3. Permanent magnet synchronous motor load density cloud and load magnetic field line distribution simulation.

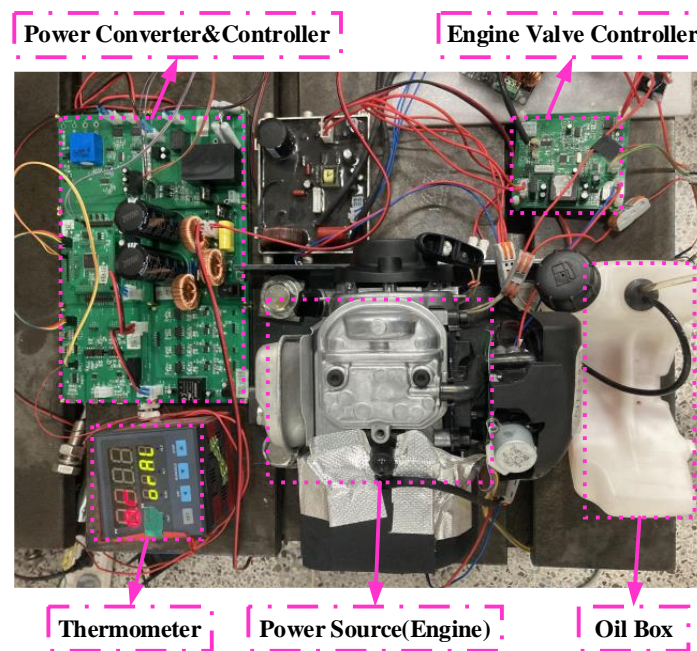


Figure A4. The actual drawing of the whole power generation system platform.

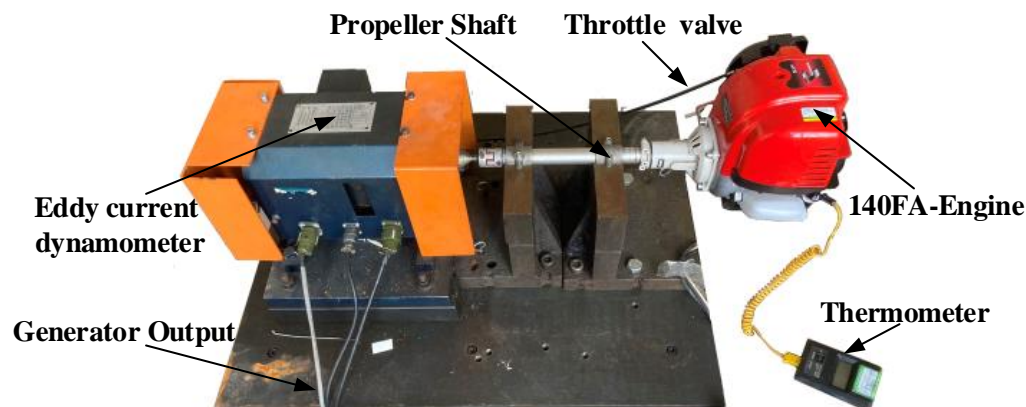


Figure A5. Engine external characteristic test platform (dynamometer platform).

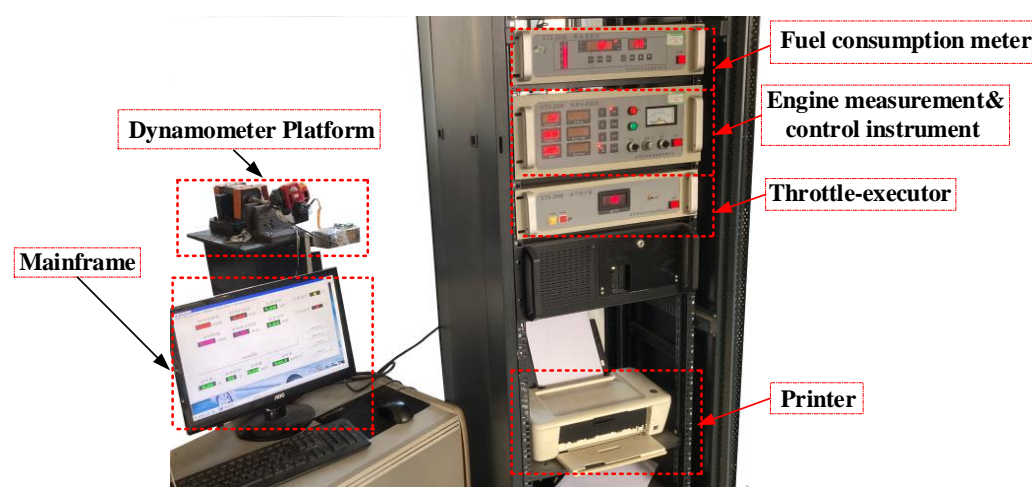


Figure A6. Engine external characteristic test platform (controller platform).

References

1. Wang, Y.; Deng, Z.; Wang, X. A Parallel Hybrid Excitation Flux-switching Generator DC Power System Based on Direct Torque Control. *IEEE Trans. Energy Convers.* **2012**, *27*, 308–317. [\[CrossRef\]](#)
2. Patin, N.; Vido, L.; Monmasson, E.; Louis, J.P.; Gabsi, M.; Lecrivain, M. Control of a Hybrid Excitation Synchronous Generator for Aircraft Applications. *IEEE Trans. Ind. Electron.* **2008**, *55*, 3772–3783. [\[CrossRef\]](#)
3. Smigins, R.; Sondors, K.; Pirs, V.; Dukulis, I.; Birzietis, G. Studies of Engine Performance and Emissions at Full-Load Mode Using HVO, Diesel Fuel, and HVO5. *Energies* **2023**, *16*, 4785. [\[CrossRef\]](#)
4. Wang, Y.; Deng, Z. Hybrid Excitation Topologies and Control Strategies of Stator Permanent Magnet Machines for DC Power System. *IEEE Trans. Ind. Electron.* **2012**, *59*, 4601–4616. [\[CrossRef\]](#)
5. Amara, Y.; Vido, L.; Gabsi, M.; Hoang, E.; Ahmed AH, B.; Lecrivain, M. Hybrid Excitation Synchronous Machines: Energy-efficient Solution for Vehicles Propulsion. *IEEE Trans. Veh. Technol.* **2009**, *58*, 2137–2149. [\[CrossRef\]](#)
6. Yuan, X.; Wang, F.; Boroyevich, D.; Li, Y.; Burgos, R. DC-link Voltage Control of a Full Power Converter for Wind Generator Operating in Weak-grid Systems. *IEEE Trans. Power Electron.* **2009**, *24*, 2178–2192. [\[CrossRef\]](#)
7. Kendouli, F.; Abed, K.; Nabti, K.; Benalla, H.; Azoui, B. High Performance PWM Converter Control Based PMSG for Variable Speed wind Turbine. In Proceedings of the Renewable Energies and Vehicular Technology Conference, Nabeul, Tunisia, 26–28 March 2012; pp. 502–507.
8. Naidu, M.; Walters, J. A 4-kW 42-V induction-machine-based Automotive Power Generation System with a Diode Bridge Rectifier and a PWM Inverter. *IEEE Trans. Ind. Appl.* **2003**, *39*, 1287–1293. [\[CrossRef\]](#)
9. Amin, M.M.N.; Mohammed, O.A. DC-bus Voltage Control Technique for Parallel-integrated Permanent Magnet wind Generation Systems. *IEEE Trans. Energy Convers.* **2011**, *26*, 1140–1150. [\[CrossRef\]](#)
10. Hui, J.C.Y.; Bakhshai, A.; Jain, P.K. An Energy Management Scheme with Power Limit Capability and an Adaptive Maximum Power Point Tracking for Small Standalone PMSG Wind Energy Systems. *IEEE Trans. Power Electron.* **2016**, *31*, 4861–4875. [\[CrossRef\]](#)
11. Camara, M.B.; Dakyo, B. Coordinated Control of the Hybrid Electric Ship Power-Based Batteries/Supercapacitors/Variable Speed Diesel Generator. *Energies* **2023**, *16*, 6666. [\[CrossRef\]](#)
12. Ahmed, T.; Nishida, K.; Nakaoka, M. Advanced Control of PWM Converter with Variable-speed Induction Generator. *IEEE Trans. Ind. Appl.* **2006**, *42*, 934–945. [\[CrossRef\]](#)

13. Fernando, W.U.N.; Barnes, M.; Marjanovic, O. Direct Drive Permanent Magnet Generator Fed AC-DC Active Rectification and Control for More-electric Aircraft Engines. *IET Electr. Power Appl.* **2011**, *5*, 14–27. [[CrossRef](#)]
14. Shen, J.X.; Miao, D.M. Machine Design and Control Strategy for Wide-speed-range PMSG Systems. *COMPEL Int. J. Comput. Math. Electr. Electron. Eng.* **2015**, *34*, 92–109. [[CrossRef](#)]
15. Schiemenz, I.; Stiebler, M. Control of a Permanent Magnet Synchronous Generator Used in a Variable Speed Wind Energy System. In Proceedings of the IEEE International Electric Machines and Drives Conference, Cambridge, MA, USA, 17–20 June 2001; pp. 872–877.
16. Khare, A.; Anabalagan, K. A Single-Stage, Multi-Port Hybrid Power Converter Integrating PV and Wind Sources for a Standalone DC System. *Energies* **2023**, *16*, 6305. [[CrossRef](#)]
17. Singh, B.; Verma, A.; Chandra, A.; Al-Haddad, K. Implementation of Solar PV-Battery and Diesel Generator Based Electric Vehicle Charging Station. *IEEE Trans. Ind. Appl.* **2020**, *56*, 4007–4016. [[CrossRef](#)]
18. Kang, L.; Chen, Y. Optimal Design of 9-Phase Permanent Magnet Synchronous Generator with Low Voltage Change Rate for Diesel Railway Vehicles. *IEEE Trans. Veh. Technol.* **2022**, *71*, 2681–2690. [[CrossRef](#)]
19. García-Pereira, H.; Blanco, M.; Martínez-Lucas, G.; Pérez-Díaz, J.I.; Sarasúa, J.-I. Comparison and Influence of Flywheels Energy Storage System Control Schemes in the Frequency Regulation of Isolated Power Systems. *IEEE Access* **2022**, *10*, 37892–37911. [[CrossRef](#)]
20. Fakhari Moghaddam Arani, M.; Mohamed, Y.A.-R.I. Cooperative Control of Wind Power Generator and Electric Vehicles for Microgrid Primary Frequency Regulation. *IEEE Trans. Smart Grid* **2018**, *9*, 5677–5686. [[CrossRef](#)]
21. Vanço, W.E.; Silva, F.B.C.; De Oliveira, M.R.; Monteiro, J.R.B.A.; De Oliveira, J.M.M. A Proposal of Expansion and Implementation in Isolated Generation Systems Using Self-Excited Induction Generator with Synchronous Generator. *IEEE Access* **2019**, *7*, 117188–117195. [[CrossRef](#)]

Disclaimer/Publisher’s Note: The statements, opinions and data contained in all publications are solely those of the individual author(s) and contributor(s) and not of MDPI and/or the editor(s). MDPI and/or the editor(s) disclaim responsibility for any injury to people or property resulting from any ideas, methods, instructions or products referred to in the content.